

Comparative Evaluation of Different Aperture Geogrids for Ballast Reinforcement through Triaxial Testing and Discrete Element Modeling

Yu Qian, University of Illinois at Urbana-Champaign, USA, yuqian1@illinois.edu
Debakanta Mishra, University of Illinois at Urbana-Champaign, USA, dmishra2@illinois.edu
Erol Tutumluer, University of Illinois at Urbana-Champaign, USA, tutumlue@illinois.edu
Jayhyun Kwon, Tensar International, USA, jkwon@tensarcorp.com

ABSTRACT

Geogrids are commonly used in transportation applications for stabilization and reinforcement due to their higher tensile strengths compared to geotextiles as well as the stiffness improvement they provide through arresting and interlocking granular particles in the geogrid apertures. Influenced by many factors, such as the aperture shape and size of geogrid, the degree of interlocking contributes significantly to the reinforcement benefit of geogrid for improving the performance of any geogrid reinforced system. This paper describes recent research efforts at the University of Illinois focused on conducting permanent deformation testing of geogrid reinforced ballast specimens using a large-scale triaxial test device. As part of the very preliminary evaluations, two different geogrids with rectangular and triangular aperture shapes were studied for reinforcement benefit of cylindrical specimens compacted and prepared with uniformly graded ballast sized aggregate materials. To further investigate the geogrid reinforcement mechanisms, an aggregate image-aided numerical modeling approach based on Discrete Element Method (DEM) was also adopted with the capability to create actual ballast aggregate particles as three-dimensional polyhedron elements having the same particle size distributions and imaging quantified average aggregate shapes and angularities. Preliminary results from both laboratory experiments and DEM simulations indicated that geogrids with triangular apertures performed more effectively in arresting particle movements through improved interlock.

1. INTRODUCTION

Geogrids are geosynthetic polymeric materials having large openings, i.e. apertures. They have been successfully used for decades in highway pavement applications, e.g., subgrade stabilization and base reinforcement. Geogrids have also been used in railroad track structures for stabilization and reinforcement purposes, especially for ballast reinforcement. Ballast is an essential layer of the railroad track structure, primarily provides drainage and load distribution. The benefit of geogrids in railway applications mainly comes from the interlocking between ballast particles and the geogrids. The degree of interlocking between geogrids and aggregate particles depends upon many factors, such as: aggregate gradation and shape properties, geogrid types and properties, compaction effort during installation, and loading conditions. Large scale triaxial tests or cyclic plate loading tests have been traditionally performed in the laboratory to evaluate the individual effects on the ballast behavior (Suiker et al. 2005, Brown et al. 2007, Anderson and Fair 2008, Aursudkij et al. 2009, Indraratna et al. 2010). Rectangular aperture geogrids with tensile strength properties in both machine and cross-machine directions have been commonly studied and recognized as useful materials that can effectively reduce the permanent deformation accumulation in the ballast under repeated loading (Bathurst and Raymond 1987, Shin et al. 2002, Raymond and Ismail 2003, Indraratna et al. 2006, Brown et al. 2007, Qian et al. 2011a). Recently, geogrids with triangular aperture shapes have also been introduced and studied for performance improvements of geogrid reinforced transportation systems (Qian et al. 2011b, Qian et al. 2012).

This paper describes preliminary findings from a research study recently initiated at the University of Illinois with the objective to conduct permanent deformation testing of geogrid reinforced ballast specimens using a large scale triaxial test device and model the micromechanical interlock behavior of geogrid-aggregate systems. Both rectangular and triangular aperture shaped geogrids were initially tested for permanent deformation behavior using a large scale triaxial testing device. To further investigate the geogrid reinforcement mechanisms, a numerical modeling approach based on Discrete Element Method (DEM) was also adopted with the capability to create actual ballast aggregate particles as three-dimensional polyhedron elements having the same particle size distributions and imaging quantified average shapes and angularities. This paper will present the laboratory test and the DEM simulation results for ballast specimens reinforced with the rectangular and triangular aperture geogrids under repeated loading.

2. REPEATED LOAD TRIAXIAL TEST OF BALLAST SPECIMENS

2.1 The University of Illinois Triaxial Ballast Tester (TX-24)

A large scale triaxial test device (The University of Illinois Triaxial Ballast Tester or TX-24) has recently been developed at the University of Illinois for testing specifically ballast size aggregate materials. The test specimen dimensions are 30.5 cm (12 in.) in diameter and 61.0 cm (24 in.) in height. The acrylic test chamber has dimensions of 61.0 cm (24 in.) in diameter and 122.0 cm (48 in.) in height. An internal load cell (Honeywell Model 3174) with a capacity of 89 kN (20 kips) is placed on top of the specimen top platen. Three vertical LVDTs are placed around the cylindrical test specimen at 120-degree angles between each other to measure the vertical deformations of the specimen from three different side locations. Another LVDT is mounted on a circumferential chain wrapped around the specimen at the mid-height to measure the radial deformation of the test specimen. Figure 1 shows the picture of a compacted and instrumented ballast specimen assembled inside the acrylic chamber ready to be transported to the loading frame.

The permanent deformation tests reported in this paper were conducted at a constant confining pressure of 34.5 kPa (5 psi) and the deviator stress applied was 172.3 kPa (25 psi). The repeated loading pattern was realistic field haversine load pulse with loading time of 0.4 seconds and 0.6-seconds of rest period between two loadings as shown in Figure 2.



Figure 1. Compacted ballast specimen with instrumentation assembled inside the acrylic chamber ready to be tested using the University of Illinois Triaxial Ballast Tester (TX-24)

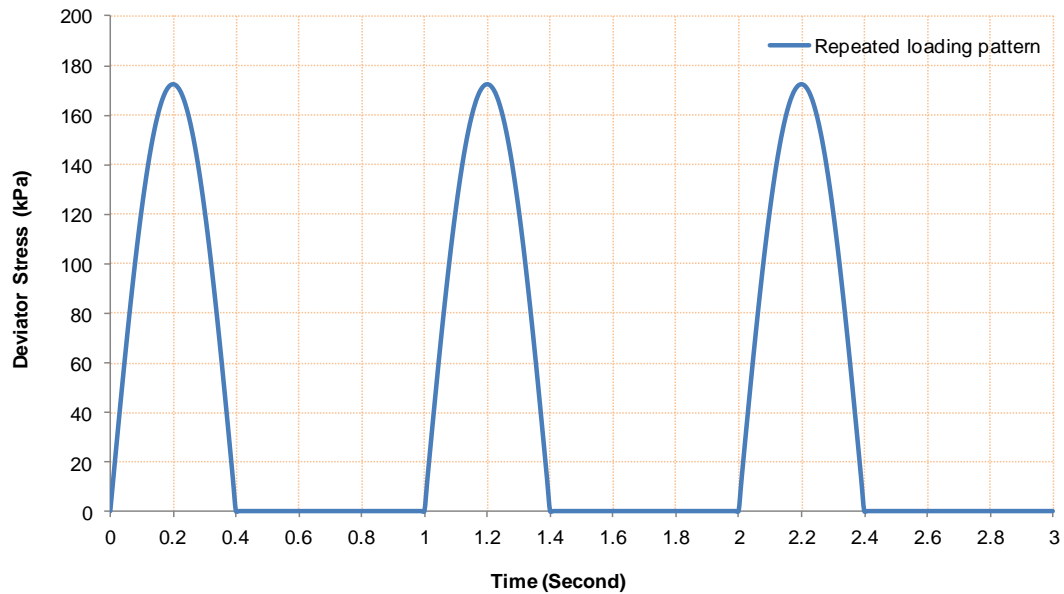


Figure 2. Repeated loading pattern used in permanent deformation tests to closely resemble field train loading

2.2 Ballast Specimen Preparation

The ballast material used in the permanent deformation tests was a clean limestone having 100% crushed aggregates. Figure 3 shows the gradation properties of the ballast material which adequately met the AREMA No.24 gradation requirements. Besides the grain size distribution, aggregate shape properties, especially the flat and elongated (F&E) ratio, the angularity index (AI), and the surface texture (ST) index, are key indices quantified by the recently enhanced University of Illinois Aggregate Image Analyzer (UIAIA) (Rao et al. 2002). One full bucket of the ballast material was scanned and analyzed using the UIAIA to determine the values of the F&E ratio, AI, and the ST index. These shape indices were then used as the essential morphological data to generate ballast aggregate particle shapes as 3D polyhedrons, i.e., individual discrete elements utilized in the ballast DEM model (see Figure 4). Table 1 lists the gradation properties and the average values of the limestone ballast shape UIAIA indices used in the DEM simulations.

An aluminum split mold was used to prepare the ballast test specimens. Three layers of a latex membrane, with a total thickness of 2.3 mm, were fixed inside the split mold and held in place by applying vacuum to prepare each specimen in layers. A thin layer of geotextile was placed on top of the base plate to prevent clogging of the vacuum port in the base plate. Approximately 68 to 73 kg (150 to 160 lbs) of ballast material was poured into the mold evenly in four lifts, with each lift compacted approximately 15-cm (6-in.) high. Each layer was compacted using a 27.2-kg (60-lb.) electric jack hammer for about 4 seconds. After compaction of the first two lifts, one layer of geogrid was placed carefully in the middle of the test specimen. At the end of placing all four lifts, each test specimen was checked for the total height and leveling of the top plate. The void ratios computed were consistently around 0.68. Figure 5 shows the photos of the geogrids tested. The detailed properties of the geogrids are given in Table 2. Figure 6 shows the aluminum split mold (on left) and the compacted ballast specimen (on right) ready for instrumentation assembly and subsequent testing.

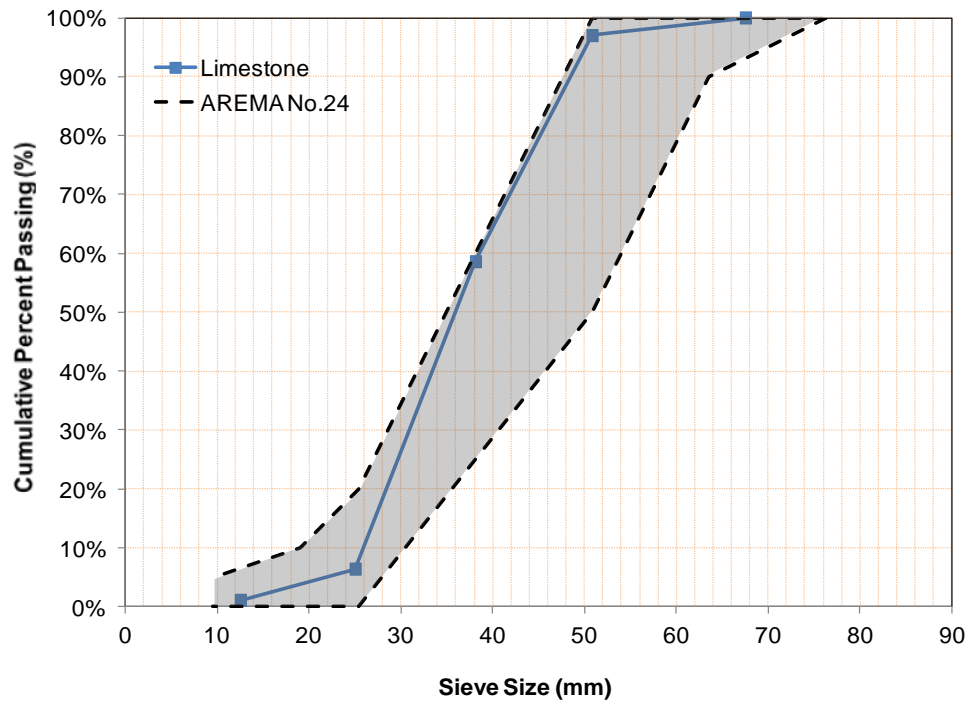


Figure3. Particle size distribution of limestone ballast aggregate compared to AREMA No. 24 specifications

Table1. UIAIA based imaging shape properties of limestone ballast material

Angularity Index (AI) in degrees	Flat & Elongation (F&E) Ratio	Surface Texture (ST)	Coefficient of Uniformity, Cu	Coefficient of Curvature, Cc
440	2.3	2	1.46	0.97

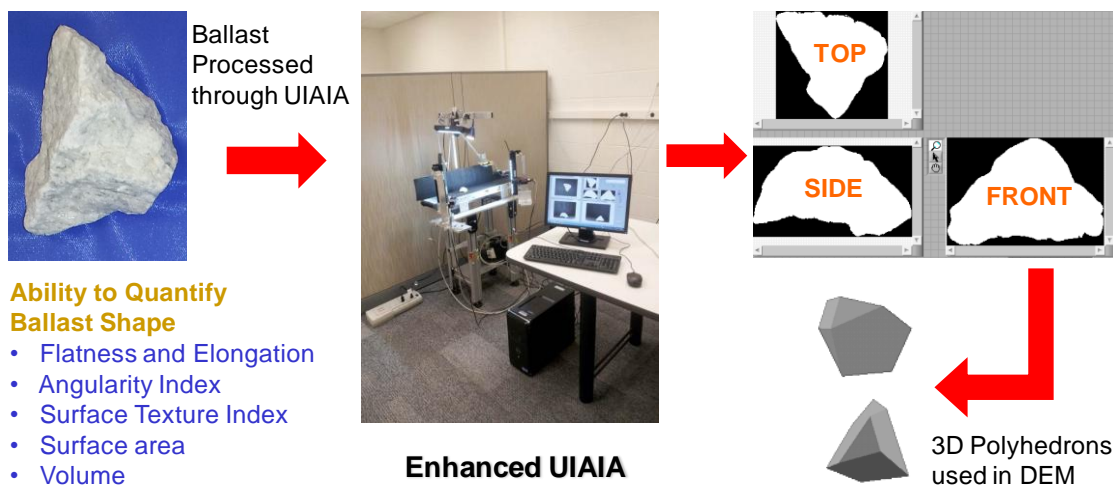
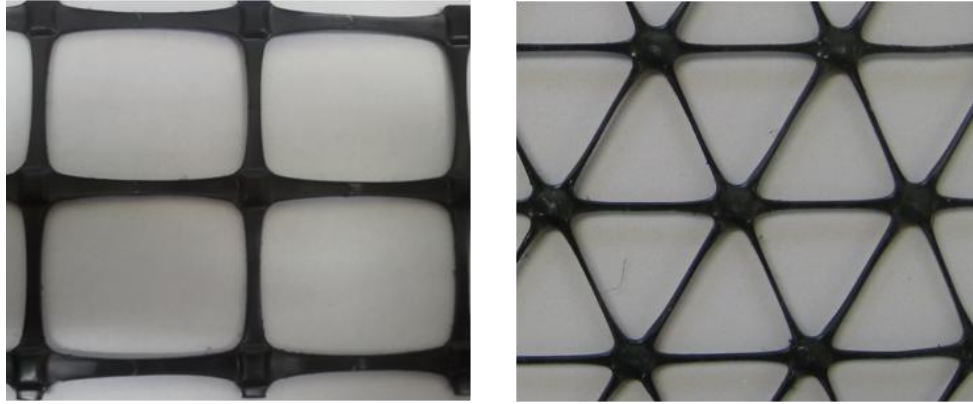


Figure4. Conceptual approach for aggregate imaging based railroad ballast discrete element model simulations



(a) Rectangular aperture geogrid (b) Triangular aperture geogrid

Figure 5. Geogrids used for ballast reinforcement in large scale triaxial tests

Table 2. Dimensions and Properties of Rectangular and Triangular Aperture Geogrids

Index Properties	Aperture Dimensions (mm)			
	Machine Direction	X-Machine Direction	Longitudinal	Diagonal
Rectangular Ap. Geogrid	46	64		
Triangular Ap. Geogrid			60	60
Minimum Rib Thickness		1.27		2.40
Mechanical Properties	Rectangular Aperture Geogrid		Triangular Aperture Geogrid	
Junction Efficiency (percentage)		93		93
Aperture Stability Modulus (m-N/deg)		0.58		
Radial stiffness (kN/m@0.5% strain)				350

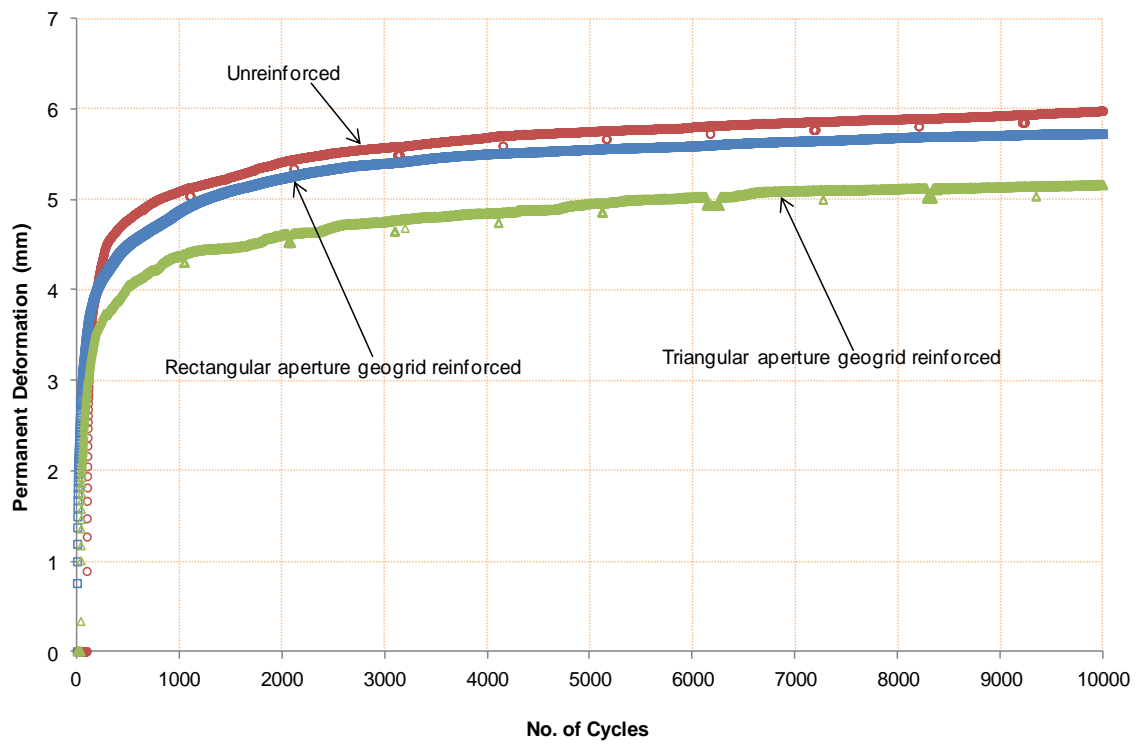


(a)

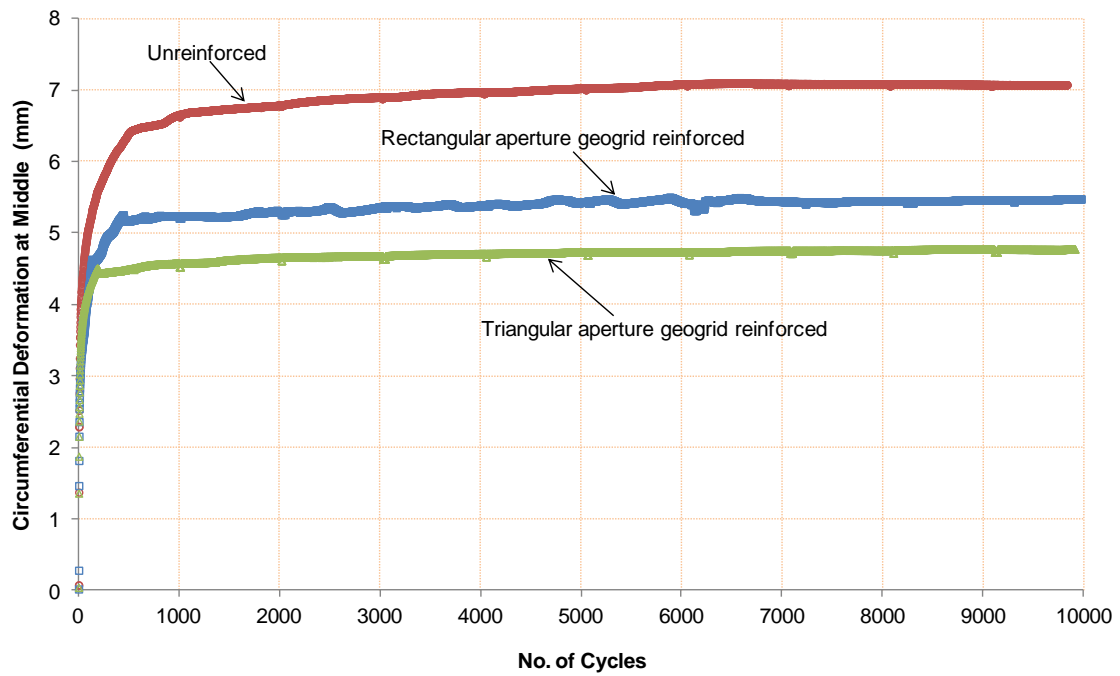


(b)

Figure 6. Pictures showing (a) Aluminum split mold used for specimen preparation, and (b) Compacted ballast specimen confined using vacuum inside three latex membranes



(a)



(b)

Figure 7. (a) Permanent axial deformation of ballast specimens; (b) Circumferential deformations of ballast specimens

2.3 Experimental Results

Figure 7 presents the preliminary results of the ballast permanent deformation tests performed in the laboratory for up to 10,000 cycles. For the first several hundreds of loading cycles, the permanent deformation and circumferential deformations increased rapidly, which was primarily due to the initial rapid “shakedown” of the ballast material. After around 1,000 loading cycles, the permanent deformation accumulated much slower and became relatively stable and so did the circumferential or radial/horizontal deformations. All the unreinforced and geogrid reinforced test specimens accumulated similar magnitudes of permanent deformation during the first one hundred load cycles and this was primarily due to the fact that geogrids were not yet fully mobilized at that time. With a single layer of geogrid placed in the middle of the test specimen, the geogrid reinforced test specimens accumulated less permanent deformation compared to the unreinforced case as the load cycles increased. When the reinforced test specimens accumulated certain amount of deformation, the geogrid’s reinforcement effect was fully mobilized and the interlock between geogrid and aggregate particles prevented further specimen bulging. This caused the specimen to stiffen and made it more resistant to deformation accumulation upon further loading. Triangular aperture geogrid reinforced test specimen accumulated the smallest permanent deformation compared with the unreinforced as well as the specimen with rectangular aperture geogrid. This indicates the triangular aperture geogrid better arrested aggregate movement with improved interlocking in all horizontal directions which can be confirmed from circumferential or radial/horizontal deformations, which happen to be of similar magnitude. Note that the triangular aperture geogrid also has thicker ribs and much higher radial stiffness when compared to the rectangular one (see Table 2). After 10,000 loading cycles, the permanent deformation for the unreinforced test specimen was 5.98 mm, the permanent deformation for the test specimen with rectangular aperture geogrid was 5.72 mm, and the permanent deformation for the test specimen with triangular aperture geogrid was 5.17 mm, respectively.

3. SIMULATION OF REPEATED LOAD TRIAXIAL TEST USING THE DISCRETE ELEMENT METHOD (DEM)

3.1 DEM Model Preparation

To investigate the mechanism of interlock and how this minimizes particle movement and causes local stiffness increase through friction and interaction of ballast particles with geogrid, a numerical modeling approach was adopted based on the Discrete Element Method (DEM) combined with image analyses of tested aggregate particles for size and shape properties. Compared to other research studies focusing on simulating triaxial tests by DEM, which often use spherical elements or element clusters (Indraratna et al. 2010, Lu and McDowell. 2010), the image-aided DEM simulation approach developed at the University of Illinois has the capability to create actual ballast aggregate particles as three-dimensional polyhedron elements having the same particle size distributions and imaging quantified average shapes and angularities. Ghaboussi and Barbosa (1990) developed the first polyhedral 3D DEM code BLOKS3D for particle flow; and Nezami et al. (2006) enhanced the program with new, fast contact detection algorithms. Tutumluer et al. (2006) combined the DEM program and the aggregate image analysis together to simulate the ballast behavior more accurately and realistically by using polyhedral elements regenerated from the image analysis results of ballast materials. This DEM approach was first calibrated by laboratory large scale direct shear test results for ballast size aggregate application (Huang and Tutumluer 2011). The calibrated DEM model was then utilized to model strength and settlement behavior of railroad ballast for the effects of multi-scale aggregate morphological properties (Tutumluer et al. 2006, 2007). More recent applications of the calibrated DEM model investigated ballast gradation (Tutumluer et al. 2009) and fouling issues (Tutumluer et al. 2008, Huang and Tutumluer 2011) that are known to influence track performance. A successful field validation study was also conducted with the ballast DEM simulation approach through constructing and monitoring field settlement records of four different ballast test sections and then comparing the measured ballast settlements under monitored train loadings to DEM model predictions (Tutumluer et al. 2011). The effect of geogrid aperture shape was recently studied by this DEM approach (Qian et al. 2011a).

Similar to the laboratory repeated load triaxial tests conducted for studying permanent deformation trends, comparative performance evaluations were also targeted for unreinforced and geogrid reinforced ballast specimens through DEM model simulations. The goal was to investigate the effects of different aperture shaped geogrids on the effectiveness of interlocking and the overall performance of the geogrid reinforced ballast. Considering the rather long DEM simulation run times that would be required for modeling the complete permanent deformation tests, the DEM simulations in this study were intended for only a small number of 100 load cycles deemed to be sufficient to enable practical comparisons of the ballast triaxial tests with or without geogrid for effectiveness within reasonable computation time. At the same time, the DEM simulation results would still help to qualitatively evaluate the influence of different aperture shapes of geogrids.

To simulate large scale repeated load triaxial compression tests using the DEM approach, the first challenge is to model the membrane which holds the specimen upright and applies the chamber confining pressure on it during testing. Previous modeling studies used rigid boundaries and chains of circular or spherical particles to simulate the membrane (Bardet 1994, Iwashita and Oda 2000, Markauskas and Kacianauskas 2006, Wang and Tonon, 2009). Lee et al. (2012)

recently used rigid rectangular cuboid discrete elements positioned in a cylindrical arrangement to simulate a flexible membrane with BLOKS3D. A similar approach was used in this study. A total of 96 rectangular cuboid discrete elements (in eight-layers) were used to form a cylindrical chamber to confine the ballast specimen as shown in Figure 7. Each layer had 12 equal size elements and the dimension of each single element was 20.32 cm (8 in.) long, 10.16 cm (4 in.) wide, and 7.62 cm (3 in.) high. These membrane elements were only allowed translational movement in radial direction. Rotation and translation movement in other directions were restricted to replicate the deformation of membrane. Note that these elements were required to have certain thickness to avoid any gap between adjacent layers when differential radial displacements between them were relatively large. Similarly, the elements were also allowed to have sufficient lengths to overlap adjacent elements to keep the circular chamber closed during simulation of triaxial tests. No contact detection was performed between these elements to allow for each element to move freely, independent of neighboring elements. The friction between the membrane elements and the ballast particles in contact with them was ignored during the DEM simulations. For the unreinforced ballast specimen, after the membrane was formed, around 500 particles were poured into the cylinder and the top platen was placed on top of the specimen to compact the ballast specimen to the same initial density under 34.5 kPa (5 psi) confining pressure as achieved in the laboratory experiment. For the geogrid reinforced ballast specimens, after the membrane was formed, about 500 particles were also poured into the cylinder in two different sets following the same gradation and shape properties of the actual ballast particles. In between, a sheet of geogrid element was generated in the middle of the ballast specimen as shown in Figure 8. The geogrid element has the same dimensions as the geogrid used in experimental study but is rigid and cannot deform. When the ballast specimen in the DEM simulation was prepared as in the similar condition as the laboratory test specimen, the repeated loading was applied to the top platen.

3.2 DEM Simulation Results

Figure 9 presents the accumulated permanent deformations as predicted by the DEM simulations for up to 100 load cycles. The deformation values at the 100th load cycle were 10.32 mm for the unreinforced case, 9.42 mm for the rectangular aperture geogrid reinforced case, and 7.97 mm for the triangular aperture geogrid reinforced case, respectively. As the purpose of the DEM simulations was to qualitatively investigate the relative performance of geogrids with different aperture shapes, due to the long DEM run times associated with each loading case, the DEM simulations for the permanent deformation predictions here considered only up to 100 cycles of the load application. Although the permanent deformations for the first hundred load cycles were somewhat similar for the unreinforced and different geogrid reinforced specimens during the laboratory testing (see Figure 7), with better control in compaction during specimen preparation in DEM simulations and the significantly high number of aggregate particle contact forces computed and checked for global granular assembly equilibrium at each iterative time step, a relatively low number of initial load cycles, such as 100 achieved here for three different simulation cases studied, was deemed to be sufficient for identifying the main reinforcement mechanisms and interlocking trends also identified in the experiments. Clearly, with DEM simulations of only up to 100 load cycles, the differences among the different ballast triaxial tests were apparent.

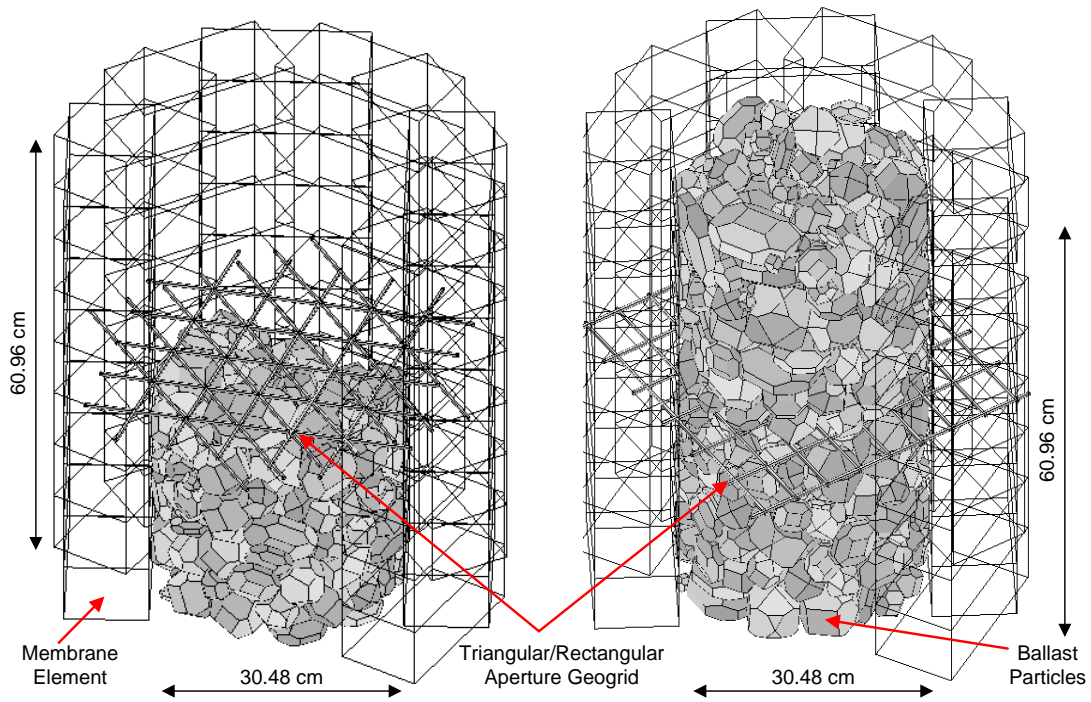


Figure8. Flexible membrane, geogrids with different apertures and ballast specimen formed in DEM simulations

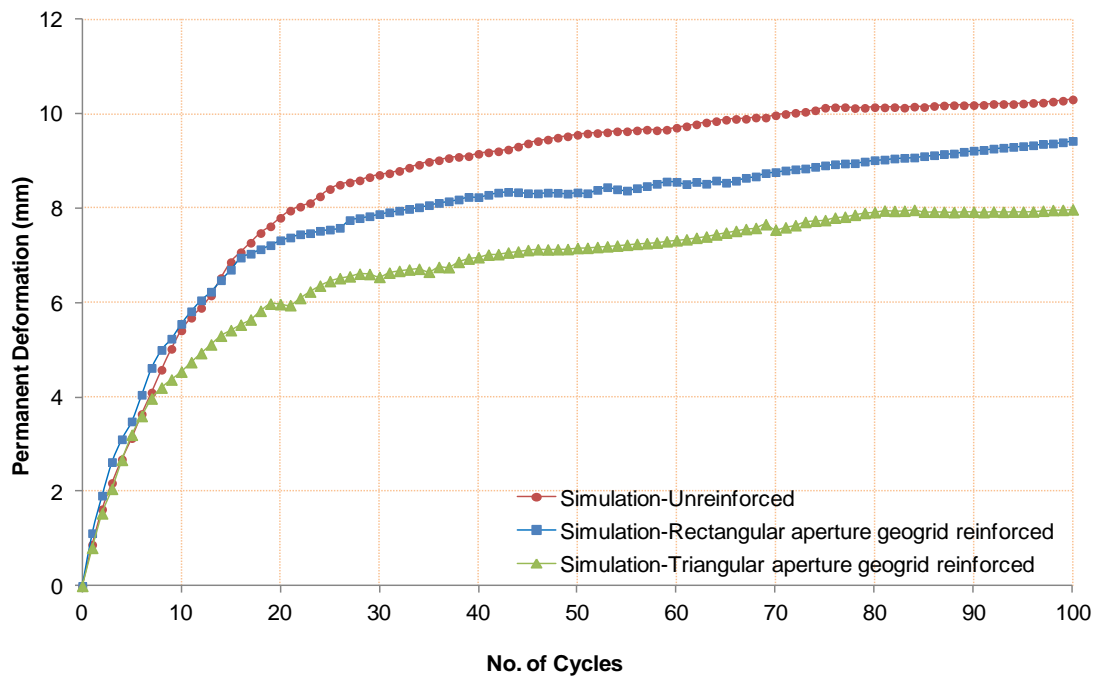


Figure9. Predicted ballast permanent deformation trends from DEM simulations with and without geogrid cases

The geogrid reinforced ballast specimens similarly yielded less permanent deformations compared to the unreinforced ballast specimen. The rectangular aperture geogrid did provide considerable reinforcement, but the triangular aperture geogrid with more uniform reinforcement in all horizontal directions provided the most significant improvement as indicated in Figure 9. These results from DEM simulations agree well with the trends observed in the

laboratory experiments. It is interesting to note that the first five DEM simulation load cycles also yielded similar magnitude deformations (approximately 4 mm) for all the unreinforced and geogrid reinforced test specimens, which means the geogrids were not fully mobilized yet. However, as the load cycles increased, the triangular aperture geogrid started to show improvement at around the 8th loading cycle during the simulation, while, the rectangular geogrid started to take effect at around the 16th loading cycle (see Figure 9). Again, the DEM simulations were intended to qualitatively compare the relative performances of geogrids with different aperture shapes using the minimum computational time. The intention has never been to match the predicted permanent deformation rates or the magnitudes at the different load cycles with the experimental results directly.

4. CONCLUSIONS

This paper focused on the permanent deformation behavior of geogrid reinforced ballast specimens as obtained from a large scale repeated load triaxial test device in the laboratory with both rectangular and triangular aperture geogrids. Further, the goal has also been to demonstrate the applicability of a repeated load triaxial testing and aggregate particle imaging based three-dimensional (3-D) numerical modeling approach, based on the Discrete Element Method (DEM), for studying geogrid-aggregate interlock reinforcement mechanism. Based on the very preliminary testing with limited data for two geogrids, the following conclusions can be drawn from this study:

1. The large scale triaxial device dedicated for testing ballast size aggregate materials developed at the University of Illinois was used successfully to investigate the permanent deformation behavior of ballast specimens under repeated loading with and without geogrid reinforcement. Both rectangular and triangular aperture geogrids were found to effectively reduce the permanent deformation accumulations of ballast materials. Triangular aperture geogrid with uniform resistance in all horizontal directions yielded the lowest permanent deformation.
2. The aggregate imaging based DEM simulation platform developed at the University of Illinois could model the repeated load triaxial tests for permanent deformation behavior of ballast specimens. Both confinement and applied deviator stress conditions on the cylindrical ballast specimens with and without geogrid reinforcement could be properly applied to investigate the interlock mechanism and micromechanical interactions between geogrids and aggregates.
3. Both the laboratory experiments and the DEM model simulations of the repeated load triaxial tests, for significantly lower number of load repetitions applied compared to the 10,000 load cycles applied in the laboratory experiments, gave similar benefits of using geogrids. The triangular aperture geogrid had better performance than rectangular aperture one in arresting particle movement in the lateral direction to yield the lowest vertical permanent deformation. More studies are needed to fully investigate aperture shape effects on the overall geogrid reinforcement mechanism.
4. The DEM simulation platform, currently being further developed, has the potential to be a quantitative tool to predict the ballast-geogrid interactions. This methodology has the potential for quantifying individual effects of various geogrid products.

ACKNOWLEDGEMENTS

The authors would like to acknowledge Tensar International, Inc. for providing the geogrids studied. The help and support of James Pforr, Research Engineer at the Illinois Center for Transportation (ICT) and Mr. Hasan Kazmee, PhD student at the Department of Civil and Environmental Engineering (CEE) at UIUC with the laboratory triaxial tests are greatly appreciated.

REFERENCES

- Anderson, W.F. and Fair, P. (2008). Behavior of Railroad Ballast under Monotonic and Cyclic Loading. *Journal of Geotechnical and Geoenvironmental Engineering*, ASCE, 134(3):316-327.
- Aursudkij, B., McDowell, G.R., and Collop, A.C. (2009). Cyclic Loading of Railway Ballast under Triaxial Conditions and in a Railway Test Facility. *Granular Matter*, (11):391-401.
- Bardet, J. P. (1994). Observations on the Effects of Particle Rotations on the Failure of Idealized Granular Materials. *Mechanics of materials*, 18(2):159-182.
- Bathurst, R. J. and Raymond, G. P. (1987). Geogrid reinforcement of ballasted track. *Transportation Research Record*. No. 1153: 8-14.
- Brown, S. F., Kwan, J. and Thom, N. H. (2007). Identifying the key parameters that influence geogrid reinforcement of railway ballast. *Geotextiles and Geomembranes*, 25(6):326-335.
- Ghaboussi J. and Barbosa R. (1990). Three-dimensional Discrete Element Method for Granular Materials. *International Journal for Numerical and Analytical Methods in Geomechanics*, (14): 451-472.

- Huang H., and Tutumluer E. (2011). Discrete Element Modeling for Fouled Railroad Ballast. *Construction and Building Materials*, (25): 3306–3312.
- Indraratna, B., Khabbaz, H., Salim, W. and Christie, D. (2006). Geotechnical properties of ballast and the role of geosynthetics in rail track stabilisation. *Journal of Ground Improvement*, 10(3): 91-102.
- Indraratna, B., Thakur, P.K., and Vinod, J.S. (2010). Experimental and Numerical Study of Railway Ballast Behavior under Cyclic Loading. *International Journal of Geomechanics*, ASCE, 10(4):136-144.
- Iwashita K., and Oda M. (2000). Micro-deformation Mechanism of Shear Banding Process Based on Modified Distinct Element Method. *Powder Technology*, 109(1-3):192-205.
- Lee, S. J., Hashash, Y.M.A., and Nezami E.G. (2012). Simulation of Triaxial Compression Test with Polyhedral Discrete Elements. *Computers and Geotechnics*, in press.
- Lu, M. and McDowell, G.R. (2010). Discrete Element Modelling of Railway Ballast under Monotonic and Cyclic Triaxial Loading. *Geotechnique*, 60(6):459-467.
- Markauskas D. and Kacianauskas R. (2006). Compacting of Particles for Biaxial Compression Test by the Discrete Element Method. *Journal of Civil Engineering and Management*, 12(2):153-61.
- Nezami E.G., Hashash, Y.M.A., Zhao D., Ghaboussi J. (2006). Shortest Link Method for Contact Detection in Discrete Element Method. *International Journal for Numerical and Analytical Methods in Geomechanics*, 30(8):783-801.
- Qian, Y., Tutumluer, E., and Huang, H. (2011a). A Validated Discrete Element Modeling Approach for Studying Geogrid-Aggregate Reinforcement Mechanisms. *Geo-Frontiers 2011*, ASCE Geo-Institute, March 13-16, Dallas, Texas.
- Qian, Y., Han, J., and Pokharel, S.K., and Parsons, R.L. (2011b). Stress analysis on triangular aperture geogrid-reinforced bases over weak subgrade under cyclic loading - an experimental study. *Journal of the Transportation Research Board*, No. 2204, Low-Volume Roads, Vol. 2, *Proceedings of the 10th International Conference on Low-Volume Roads*, July 24–27, Lake Buena Vista, Florida, USA, 83-91.
- Qian, Y., Han, J., and Pokharel, S.K., and Parsons, R.L. (2012). Performance of Triangular Aperture Geogrid-Reinforced Base Courses over Weak Subgrade under Cyclic Loading. *Journal of Materials in Civil Engineering*, in press.
- Rao, C., Tutumluer, E. and Kim, I.T. (2002). Quantification of Coarse Aggregate Angularity Based on Image Analysis. *Transportation Research Record*. No. 1787, 193-201.
- Raymond, G. and Ismail, I. (2003). The effect of geogrid reinforcement on unbound aggregates. *Geotextiles and Geomembranes*, 21(6): pp.355-380.
- Shin, E. C., Kim, D. H. and Das, B. M. (2002). Geogrid-reinforced railroad bed settlement due to cyclic load. *Geotechnical and Geological Engineering*, 20:261-271.
- Suiker, A. S. J., Selig, E. T., and Frenkel, R. (2005). Static and Cyclic Triaxial Testing of Ballast and Subballast. *Journal of Geotechnical and Geoenvironmental Engineering*, ASCE, 131(6): 771-782.
- Tutumluer, E., Huang, H., Hashash, Y.M.A., and Ghaboussi, J. (2006). Aggregate Shape Effects on Ballast Tamping and Railroad Track Lateral Stability. In *Proceedings of the AREMA Annual Conference*, Louisville, Kentucky, USA, September 17-20.
- Tutumluer, E., Huang, H., Hashash, Y.M.A., and Ghaboussi, J. (2007). Discrete Element Modeling of Railroad Ballast Settlement. In *Proceedings of the AREMA Annual Conference*, Chicago, Illinois, September 9-12.
- Tutumluer, E., Huang, H., Hashash, Y.M.A., and Ghaboussi, J. (2009). AREMA Gradations Affecting Ballast Performance Using Discrete Element Modeling (DEM) Approach. In *Proceedings of the AREMA Annual Conference*, Chicago, Illinois, September 20-23.
- Tutumluer, E., Huang, H., Hashash, Y.M.A., and Ghaboussi, J. (2008). Laboratory Characterization of Coal Dust Fouled Ballast Behavior. In *Proceedings of the AREMA Annual Conference*, Salt Lake City, Utah, September 21-23.
- Tutumluer, E., Qian, Y., Hashash, Y.M.A., Ghaboussi, J., and David, D.D. (2011). Field Validated Discrete Element Model for Railroad Ballast. In *Proceedings of the AREMA Annual Conference*, Minneapolis, Minnesota, September 18-21.
- Wang, Y. and Tonon, F. (2009). Modeling Triaxial Test on Intact Rock Using Discrete Element Method with Membrane Boundary. *Journal of Engineering Mechanics*, 135(9):1029-1037.